Observation of multiple higher-order stopgaps from three-dimensional chalcogenide glass photonic crystals

Elisa Nicoletti,[1] Guangyong Zhou,[1] Baohua Jia,[1] Michael James Ventura,[1] Douglas Bulla,[2] Barry Luther-Davies,[2] and Min Gu[1,*]

[1]*Centre for Micro-Photonics and Centre for Ultrahigh-Bandwidth Devices for Optical Systems (CUDOS), Faculty of Engineering and Industrial Sciences, Swinburne University of Technology, P.O. Box 218 Hawthorn, 3122 Victoria, Australia*

[2]*Laser Physics Centre and CUDOS, Research School of Physical Sciences and Engineering, Australian National University, Canberra ACT 0200, Australia*

**Corresponding author: mgu@swin.edu.au*

Received June 30, 2008; revised August 28, 2008; accepted August 28, 2008; posted September 8, 2008 (Doc. ID 98131); published October 9, 2008

For the first time to our knowledge the observation of near-IR multiple higher-order stopgaps in three-dimensional photonic crystals (PhCs) fabricated using the direct-laser-writing method in thick chalcogenide glass films is reported. The fabrication and etching conditions necessary to realize well-defined structures are presented. The fabricated PhCs exhibit higher-order stopgaps, which are only evident in high-quality structures. The higher-order stopgaps observed permit these high-refractive-index and high-nonlinear PhCs to be used directly as functional photonic devices operating at telecommunication wavelengths without further miniaturizing structural dimensions. © 2008 Optical Society of America

OCIS codes: 220.4000, 160.5298, 050.6624.

Photonic crystals (PhCs) are one of the key components in the next generation of miniaturized photonic devices because of their capability to control and manipulate the flow of light on a wavelength scale [1,2]. Photosensitive chalcogenide glasses (ChGs) have recently been utilized as a unique building block for three-dimensional (3D) PhCs because of their high refractive index, high nonlinearity, and high transparency in the near- to mid-IR region. Such properties are essential to open 3D complete bandgaps with wavelength tunability [3–5]. Although several methods have been proposed to achieve 3D PhCs with ChGs [3,4,6], direct laser writing (DLW) using a femtosecond-laser-induced multiphoton process is the most convenient, efficient, and flexible approach to generate arbitrary PhCs with functional stopgaps [4]. Combining the nonlinear nature of the fabrication process with a threshold mechanism, a resolution limit of a couple of hundred nanometers can be achieved, which could lead to a stopgap in the near-infrared (NIR) wavelength range ($>2.2\ \mu$m). However, further miniaturizing the structures to obtain a stopgap in the telecommunication wavelength region is challenging owing to the high refractive indices of ChGs (>2.3). Utilizing higher-order gaps have been proven to be an effective alternative approach to achieve high-frequency stopgaps without structural miniaturization of PhCs [7]. In fact, higher-order stopgaps in polymer PhCs have been recently demonstrated to be successfully used in controlling the spontaneous emission from quantum dots in the telecommunication wavelength range [8]. However, the generation of PhCs with controllable higher-order stopgaps is nontrivial and so far, to the best of our knowledge, have not yet been achieved in ChG-based 3D PhCs. To observe higher-order stopgaps, high-quality structures with minimum defects are required. As such, a thorough investigation of the fabrication conditions in thick ChG films is a prerequisite to obtain structures that exhibit deep stopgaps.

In this Letter, for the first time to our knowledge, we report on the observation of multiple higher-order stopgaps in the NIR wavelength region in 3D ChG PhCs fabricated using the DLW technique. The fabrication conditions as well as the etching process were investigated in detail to find the optimized structural arrangement necessary to generate higher-order stopgaps. A minimum feature size of 150 nm has been demonstrated, which is far beyond the diffraction limit and comparable to the fabrication limit achievable in photosensitive polymers [9].

A similar experimental setup to that used in two-photon-polymerization (2PP) experiments was employed for PhC fabrication in ChGs [10,11]. A beam of a Ti:sapphire laser (wavelength 800 nm, repetition rate 1 kHz, Spitfire) was tightly focused using a high NA (NA=1.4, 100×, Olympus) oil immersion objective into a $\sim$16–20-μm-thick As_2S_3 film mounted onto a 3D piezoelectric scanning stage. The film was prepared from stoichiometric As_2S_3 bulk glass (Amorphous Materials Inc.) using thermal evaporation from a temperature controlled Ta baffled boat in a vacuum chamber pumped to a base pressure of 2×10^{-7} Torr and at a temperature of 310°C. Films were deposited onto glass slide substrates held in a carousel with a planetary rotation on the top of the chamber at room temperature with a deposition rate of $\sim$6 Å/s. Films prepared in this manner have an approximate refractive index of 2.35 and different bond structures from the bulk glass. Raman spectroscopy [12] has shown that As_2S_3 films contain disconnected molecular cagelike structures (As_4S_4, As_4S_6, etc.) that form in the vapor phase and are then frozen into the deposited film. These molecular cages are

0146-9592/08/202311-3/$15.00

metastable and can "open" when thermally or optically excited leading to rebonding and polymerization of the glass network. Using a femtosecond laser beam it is possible to induce structural modification in a highly localized area of the glass through a two-photon-induced nonlinear process at wavelength 800 nm [13].

The unpolymerized glass is removed using a solution of diisopentylamine (Alfa Aesar) and dimethylsulfoxide (Sigma-Aldrich). The removal of the unpolymerized glass was undertaken in multiple steps, starting with a highly concentrated solution (2–3 mol.%) for about 5 min, followed by immersions in a solution of lower concentration (0.5–1 mol.%) for 10 min. This allows the accurate control of the etching process to obtain high-quality 3D porous microstructures.

To find out the resolution limit of the fabrication process, the threshold fabrication mechanism was introduced [9,11]. A systematic study of the fabrication conditions was conducted by fabricating two-dimensional (2D) lines [Fig. 1 (right panel)] at different laser powers while the scanning speed was kept constant at 50 μm/s. A plot of the lateral thicknesses of these lines as a function of the laser power shows a clear threshold feature (Fig. 1). For the first time rods with 150 nm in thickness and excellent mechanical strength have been successfully achieved. This resolution limit is comparable to that of the 2PP technique in polymer [9] and can be attributed to the threshold fabrication technique in combination with our multistep etching process.

To generate functional 3D PhCs, thick (20 μm) ChG films are essential. This allows the formation of sufficient layers in the stacking direction. The particular geometry we are interested in is a woodpile structure [9–11]. With a given thickness of 20 μm, approximately 16 layers can be fabricated depending on the layer spacing (dz). In Fig. 2(a), a scanning electron microscopy (SEM) image of a 16-layer woodpile PhC with an in-plane spacing (dx) of 1 μm and $dz=1.2$ μm is presented. Two walls were fabricated to support the structure during the etching process. A highly magnified image of the structure is presented

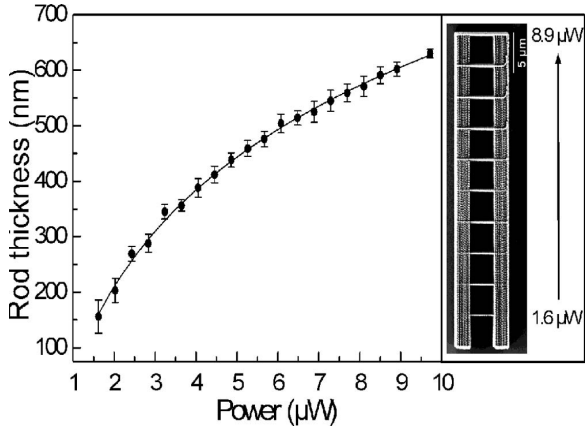

Fig. 1. Experimental plot of the lateral rod dimension versus the laser power. The right panel shows an SEM image of the 2D rods fabricated at different powers (from 1.6 to 8.9 μW). Scale bar, 5 μm.

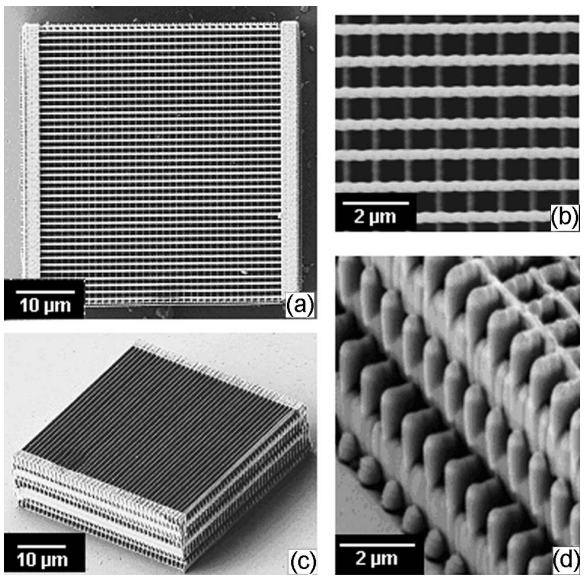

Fig. 2. SEM images of As_2S_3 woodpile structures. (a) and (b) Top views. (c) and (d) Side views.

in Fig. 2(b) in which a rod thickness of less than 200 nm can be identified. The surfaces of the rods are smooth, although some modulations are observed. The side view of the entire PhC is highlighted in Figs. 2(c) and 2(d). Neither shrinkage nor expansion is observed. Figure 2(d) shows a magnified image of the cross sections of the rods. The ellipsoidal shape is a consequence of the strong spherical aberration induced by the large refractive index mismatch between the immersion oil and the ChG. A mean aspect ratio of 4.46 was found after a primary compensation for the aberration by setting multilevel fabrication powers at different depths.

Figure 3 (left panel) shows the calculated band diagram of the structure presented in Fig. 2, accom-

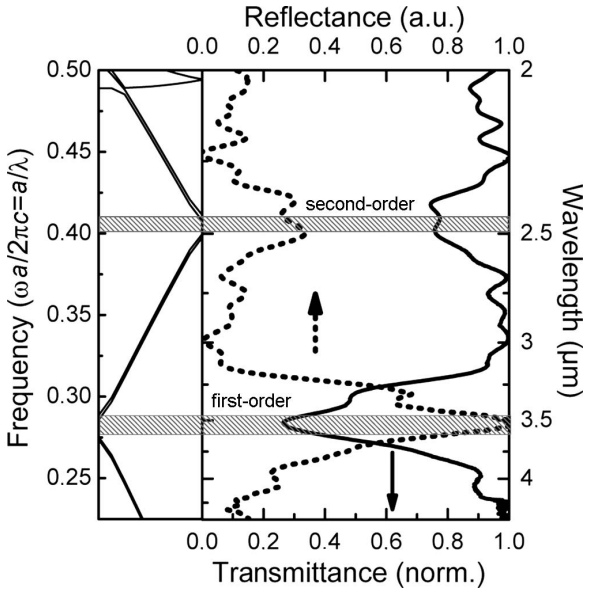

Fig. 3. Left, calculated band structure of a 3D woodpile PhC predicating the presence of both the first- and the second-order stopgaps. Right, measured transmission and reflection spectra of the 3D woodpile PhC matching exactly the calculation.

plished using commercially available R-SOFT software. Owing to the ellipsoidal shape of each rod and the geometry of the woodpile structure (face-centered tetragonal), no complete bandgap could be achieved. Only a partial bandgap can be observed in the stacking direction ($G-Y$). However, the calculation predicts that not only a first-order stopgap (at normalized frequency 0.28–0.29), but also a higher-order gap (at frequency 0.40–0.41) exists in the PhCs. The baseline corrected Fourier-transform IR spectra measured in the stacking direction, presented in Fig. 3 (right panel), confirm the calculation by showing two pronounced dips (peaks) in the transmission (reflection) spectrum at the exact wavelengths predicted by plane-wave theory. The first gap at wavelength 3.5 μm has a 74% suppression ratio in transmission while the higher-order gap shows 25% suppression. The presence of a higher-order stopgap is clear evidence of the highly defined woodpile structure. The PhCs fabricated here provide an effective alternative to structural miniaturization as a means to achieve stopgaps in a shorter wavelength region.

Further calculations reveal that the multiorder stopgaps could be engineered and tuned by either changing the filling ratio or the lattice constant of the PhCs. To confirm this, a series of PhCs were fabricated with the same lattice parameters ($dx=1$ and $dz=0.96$ μm) by varying the laser power. This is analogous to changing the filling ratio of the resultant PhC structures. The baseline corrected transmission spectra are shown in Fig. 4(a). In all cases the first-order and the second-order stopgaps can be clearly identified. Increasing the laser power from 4 to 7.2 μW, at an interval of 0.8 μW, the position of the first-order stopgap predictably shifts to longer wavelengths. The dependence of the stopgap position on the fabrication laser power is plotted in Fig. 4(b). As expected, the central wavelengths of both the first- and the second-order stopgaps concomitantly increase as the laser power is increased. Alternatively, the tuning of the multiorder stopgaps can be realized by changing the lattice constant of the PhCs, as shown in Fig. 4(c), in which the stopgap of a series of PhCs fabricated at the same power level (6.5 μW) is plotted as a function of dz. The stopgap wavelengths of both the first- and the second-order stopgaps show a linear dependence on the laser power as well as the lattice constant.

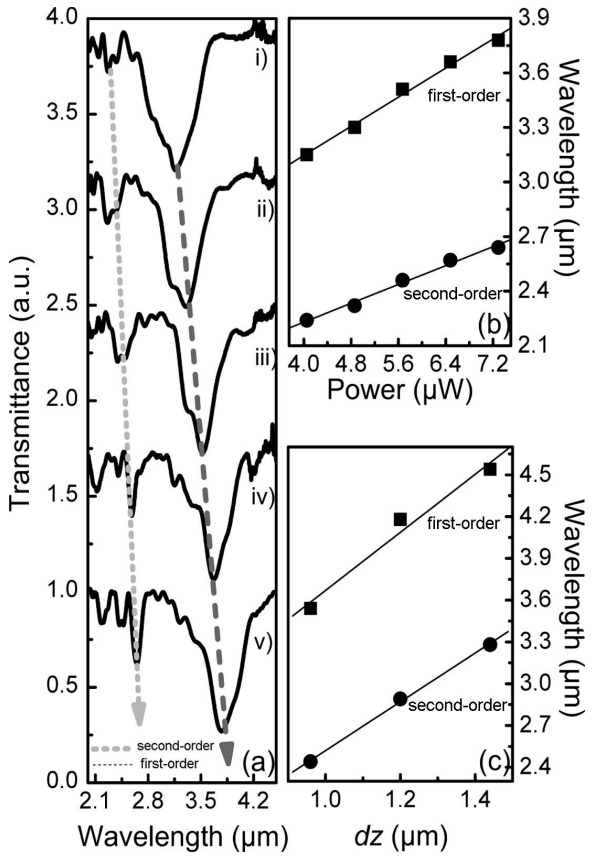

Fig. 4. (a) Transmission spectra of 3D woodpile PhCs with the same in-plane spacing $dx=1$ μm and interlayer spacing $dz=0.96$ μm but different fabrication powers: (i) 4.0, (ii) 4.8, (iii) 5.6, (iv) 6.4, (v) 7.2 μW. Stopgap position of both the first- and the second-order stopgaps versus the (b) fabrication power and (c) layer spacing dz.

In conclusion, using DLW, combined with a multistep etching process, high-quality 3D PhCs with large NIR stopgaps have been fabricated in thick ChGs. For the first time to our knowledge multiorder stopgaps have been observed and engineered in high-refractive 3D ChG PhCs. The fabricated structures provide an effective alternative to achieve photonic bandgaps in the telecommunication wavelength region, circumventing the need for structural miniaturization of the PhCs. Thus exciting applications, for example controlling the spontaneous emission [8], can be enabled in such high-refractive-index PhCs at this important wavelength region.

This work was produced with the assistance of the Australian Research Council (ARC) under its Centers of Excellence program. CUDOS (the Centre for Ultrahigh-Bandwidth Devices for Optical Systems) is an ARC Centre of Excellence.

References

1. J. D. Joannopoulos, R. D. Meade, and J. N. Winn, *Photonic Crystals* (Princeton U. Press, 1995).
2. S. Noda, K. Tomoda, N. Yamamoto, and A. Chutinan, Science **289**, 604 (2000).
3. A. Feigel, Z. Kotler, B. Sfeza, A. Arsh, M. Klebanov, and V. Lyubin, Appl. Phys. Lett. **77**, 3221 (2000).
4. S. Wong, M. Deubel, F. Perez-Willard, S. John, and G. A. Ozin, Adv. Mater. **18**, 265 (2006).
5. A. Zakery and S. R. Elliot, J. Non-Cryst. Solids **330**, 1 (2003).
6. B. H. Juarez, S. Rubio, J. Sanchez-Dehesa, and C. Lopez, Adv. Mater. **14**, 1486 (2002).
7. M. Straub, M. Ventura, and M. Gu, Phys. Rev. Lett. **91**, 043901 (2003).
8. M. Ventura and M. Gu, Adv. Mater. **20**, 1329 (2008).
9. J. Serbin and M. Gu, Adv. Mater. **18**, 221 (2006).
10. M. Straub and M. Gu, Opt. Lett. **27**, 1824 (2002).
11. B. Jia, J. Li, and M. Gu, Aust. J. Chem. **60**, 484 (2007).
12. A. Schulte, C. Rivero, K. Richardson, K. Turcotte, V. Hamel, A. Villeneuve, T. Galstain, and R. Vallee, Opt. Commun. **198**, 125 (2001).
13. C. Meneghini and A. Villeneuve, J. Opt. Soc. Am. B **15**, 2946 (1998).